Robustness Verification of High Precision Space Reflector Structural System Using Robust Multiobjective Optimization

Robustness Verification of High Precision Space Reflector Structural System Using Robust Multiobjective Optimization

By Ryo KODAMA[1)], Nozomu KOGISO[1)] and Hiroaki TANAKA[2)]

[1)]*Department of Aerospace Engineering, Osaka Prefecture University, Sakai, Japan*
[2)]*Department of Aerospace Engineering, National Defence Academy of Japan, Yokosuka, Japan*

A high precision space structural system will not allow even a thermal deformation on orbit. Under such design requirement, new uncertainty estimation method is required. The objective of this research is to establish a new design methodology to overcome a conventional budget allocation method. One strategy is to apply the robust multiobjective optimization method. Recently, we develop the robust multiobjective optimization method that the mean performance and its variation are modelled as individual objective functions. Then, the effect of uncertainty on the performance is visualized through Pareto solutions. Through numerical examples of the space reflector model, Pareto solutions are obtained from the two-objective and then the three-objective function problems. Then, the effects of variations of several physical parameters on the surface shape error and the robustness are discussed.

Key Words: High Precision Space Structure, Uncertainty, Robust Multiobjective Optimization, Satisficing Trade-Off Method

1. Introduction

Space antenna for space exploration missions require large aperture areas and high surface shape accuracy, as well as lightweightness. The radial rib and hoop cable structure for the space reflector, as illustrated in Fig. 1 [1)-3)] , was proposed to satisfy these difficult requirements. The ribs are arranged in the radial direction from a central hub, hoop cables are connected to the radial ribs and arranged concentrically, and tie cables are connected between the rib and the backup deployable truss. The ribs are deformed to the ideal parabola shape by cable tension upon deployment, where they were originally straight form folding.

The structural design is verified through the one-dimensional rib model shown in Fig. 2 [2)] . The one-dimensional model consists of a single rib taken from the whole reflector and a cable element that represents the tie cable. The root of the rib is simply supported, and the lower end of the tie cable is fixed in the vertical direction and free to move in the longitudinal direction. The hoop cable tension is modeled as a concentrated nodal load that deforms the rib into the ideal parabola shape from the original straight form. The deformation transfers the tension force to the tie cable as a reaction force.

The structural design problem is to determine the rib stiffness distribution to minimize the RMS error between the ideal parabola shape and the rib deformation shape under the given applied loads that is evaluated by nonlinear finite element method. The design problem can be formulated as the optimization problem, where the rib dimension and the natural length of the tie cable are treated as design variables. In addition, this study investigates the effect of the cable tensions on the rib deformation as well as the RMS error minimization design. Under actual situation, material property or the applied load has uncertainly, that will make the rib deformation changed from the ideal shape. When the deformation shape is varied from the ideal shape, it is necessary to adjust the deformation by changing the cable tensions. However, the RMS error sensitivity with respect to the cable tension makes smaller for the cables that is not used for the adjuster for the robustness.

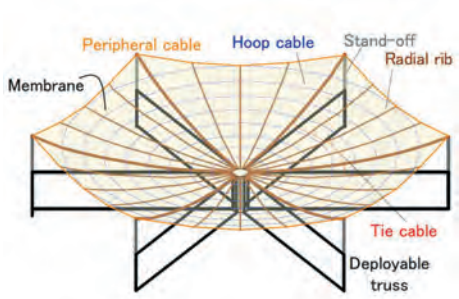

Fig. 1. Radial-rib/hoop cable reflector structure

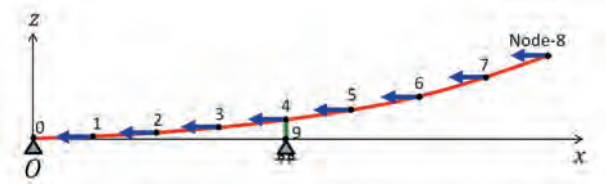

Fig. 2. Simplified one-dimensional structural model of the rib/cable reflector

The objective of this study was to investigate the design problem, especially the trade-off between the RMS error and the RMS sensitivity with respect to the cable tension. For this purpose, the design problem was formulated as a multiobjective optimization problem. Then, the trade-off analysis was performed by investigating the Pareto set distributions. This study adopted the satisficing trade-off method (STOM) [4)] as the multiobjective optimization method. STOM can obtain a single, highly accurate Pareto solution, regardless of the shape of the Pareto set. Therefore, the method is widely applied to engineering design problems [5), 6)] . Some of the authors developed robust and reliability-based multiobjective optimization methods considering uncertainty using STOM [7), 8)] . By introducing an aspiration level that corresponds to the user's preference for each objective function, STOM transforms the multiobjective optimization problem into an equivalent single-objective problem. Mathematical programming techniques can be applied to

the transformed problem, meaning that STOM obtains a Pareto solution efficiently. In addition, a highly diverse and uniformly distributed Pareto set can be obtained by parametrically changing the aspiration level. STOM is an interactive approach because the search process is repeated by changing the aspiration level until the user is satisfied with the solution. The automatic trade-off analysis method [9] is one approach of updating the aspiration level using sensitivity information.

On the multiobjective optimization, it is also important to select the suitable design candidate among the Pareto set. Conventional methods evaluate the trade-off relationship after obtaining all possible Pareto solutions. On the other hand, in this study, the range of design candidates is narrowed interactively by increasing the number of objective functions as follows. Primary objective of the design is to satisfy the RMS error limit of the rib deformation. At first, the RMS error minimized design is obtained as a reference design by a single objective optimization. Then, the multiobjective optimization is applied to investigate the trade-off relationship between the RMS error and its sensitivity with respect to the tie cable tensions. Where, the RMS error and its sensitivity with respect to the tie cable tension or the outermost hoop cable tension are used as the two objective functions. Uniformly distributed Pareto set in each two objective optimization problem is obtained by parametrically changing the aspiration level. Through the trade-off analysis, the design range is narrowed to the interested range. Then, the three objective optimization problem including RMS error and both sensitivities is performed to set the aspiration level only in the interesting design range. Finally, the trade-off analysis is performed through obtained small numbers of Pareto solutions. This approach is applied to the the robust design that minimizes the three objective functions; RMS error and its sensitivity. strategies.

2. Multiobjective Optimal Design

A multiobjective optimization problem is an optimization problem with multiple objective functions as follows.

$$\boldsymbol{f}(\boldsymbol{x}) = [f_1(\boldsymbol{x}), f_2(\boldsymbol{x}), \cdots, f_k(\boldsymbol{x})]^T \tag{1}$$

where k is the number of objective functions, $\boldsymbol{x} = (x_1, x_2, \cdots, x_n)^T$ are the design variables, and n is the number of design variables.

The multiobjective optimization problem is generally formulated as follows:

$$\begin{aligned} \text{Minimize:} \quad & \boldsymbol{f}(\boldsymbol{x}) = [f_1(\boldsymbol{x}), f_2(\boldsymbol{x}), \cdots, f_k(\boldsymbol{x})]^T \\ \text{subject to:} \quad & g_j(\boldsymbol{x}) \le 0 \quad (j = 1, \cdots, m) \\ & x_i^L \le x_i \le x_i^U \quad (i = 1, \cdots, n_x) \end{aligned} \tag{2}$$

where $g_j(\boldsymbol{x})$ $(j = 1, \cdots, m)$ are constraint conditions and x_i^U and x_i^L are the upper and lower limits of the design variables, respectively.

2.1. Satisficing Trade-off Method (STOM)

STOM is known to be an interactive optimization method that converts a multiobjective optimization problem into the equivalent single-objective optimization problem by introducing an aspiration level that corresponds to the user's preference for each objective function value. The flow of the STOM is summarized in Fig. 3 and briefly described as follows.

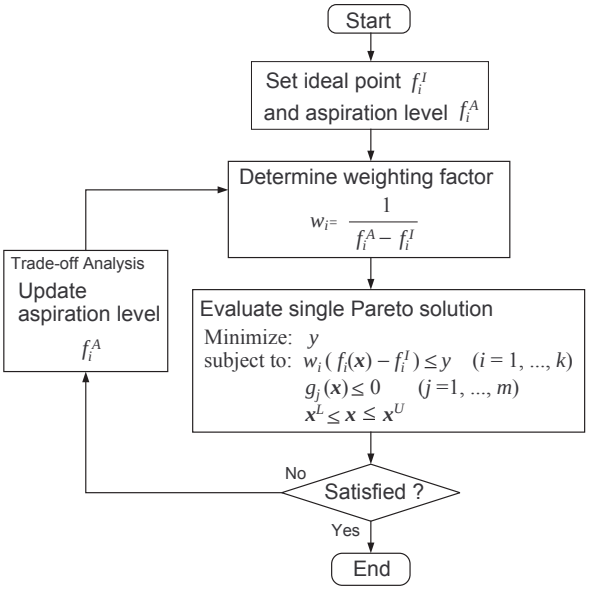

Fig. 3. Flowchart of STOM

Step 1 Set the ideal point f_i^I, $(i = 1, \cdots, k)$ of each objective function. The ideal point is usually determined by solving a single-objective optimization problem considering only the corresponding objective function, $f_i(\boldsymbol{x})$. The ideal point for the mean performance is obtained by solving the deterministic design problem. As an alternative, the ideal solution without solving the optimization problem can be used such as zero to the ideal point for the standard deviation.

Step 2 Set the aspiration level f_i^A, $(i = 1, \cdots, k)$ of each objective function and evaluate the weight coefficient, w_i, as follows:

$$w_i = \frac{1}{f_i^A - f_i^I} \quad (i = 1, \cdots, k) \tag{3}$$

Step 3 Formulate the multiobjective optimization problem in Eq. (2) into the weighted Tchebyshev norm problem as follows:

$$\begin{aligned} \text{Minimize:} \quad & \max_{i=1,\cdots,k} w_i \left(f_i(\boldsymbol{x}) - f_i^I \right) \\ \text{subject to:} \quad & g_j(\boldsymbol{x}) \le 0 \quad (j = 1, \cdots, m) \\ & x_i^L \le x_i \le x_i^U \quad (i = 1, \cdots, n_x) \end{aligned} \tag{4}$$

Step 4 The min-max problem in Eq. (4) is transformed into the equivalent single-objective problem by introducing a slack design variable y as follows:

$$\begin{aligned} \text{Minimize:} \quad & y \\ \text{subject to:} \quad & w_i \left(f_i(\boldsymbol{x}) - f_i^I \right) \le y \quad (i = 1, 2, \cdots, k) \\ & g_j(\boldsymbol{x}) \le 0 \quad (j = 1, \cdots, m) \\ & x_i^L \le x_i \le x_i^U \quad (i = 1, \cdots, n) \end{aligned} \tag{5}$$

When Eq. (5) is solved using a nonlinear programming method such as a sequential programming method, an accurate Pareto optimal solution is obtained in comparison with an evolutionary method.

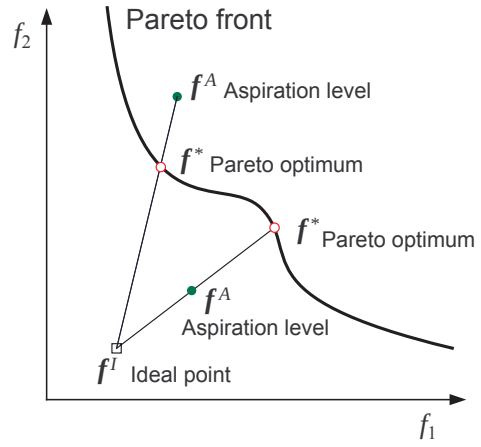

Fig. 4. Pareto solution search process of STOM described in the objective function space

Table 1. Rib natural length and cable tension for the simplified structural model shown in Fig. 2

(a) Rib properties

Section	0-1	1-2	2-3	3-4
Natural length (m)	0.25254	0.25279	0.25327	0.25400
Section	4-5	5-6	6-7	7-8
Natural length (m)	0.25500	0.25620	0.25760	0.25930

(b) Hoop cable tension applied at nodal force to the left direction

Node	1	2	3	4
Load[N]	-0.4187	-1.0467	-1.0467	-1.0467
Node	5	6	7	8
Load[N]	-1.0467	-1.0467	-2.0934	-2.0934

Step 5 If the objective function values are satisfactory, the search is completed. Otherwise, update the aspiration level f_i^A and return to Step 2. The automatic trade-off analysis method [9] is one of the methods used to reasonably update the aspiration level.

The weight coefficient, w_i, plays an important role in obtaining the Pareto solution in the direction of the aspiration level, which is directly related to the designer's preference. As shown in Fig. 4, the Pareto optimal solution is usually located on the line connecting the ideal point and the aspiration level in the objective function space, regardless of whether or not the aspiration level lies in the feasible region. On the other hand, the optimal solution is often not located on the line when some constraints are active. In that case, designers can investigate the effect of the active constraints on the Pareto optimal solution. An accurate Pareto set is obtained by parametrically changing the aspiration level. Designers can investigate the desired region in detail only by arranging the aspiration level properly without obtaining the full Pareto set.

3. Design Problem

The original design problem [2] was formulated as a deterministic optimization problem in order to determine the rib thickness distribution under the prescribed tension. In this study, the two-dimensional simple model shown in Fig. 2 is used to evaluate the deformation shape by a nonlinear finite element method.

Table 2. Deterministic optimal solution and side constraints for RMS error minimization design

(a) Rib thickness

Position	0-0.5	0.5-1	1-2	2-3	3-4
Lower limit (mm)	2.5	3.0	4.0	4.0	4.0
Optimum height (mm)	2.96	3.87	4.84	5.50	5.96
Position	4-5	5-6	6-7	7-7.5	7.5-8
Lower limit (mm)	4.0	4.0	4.0	2.5	2.0
Optimum height (mm)	5.85	5.12	4.13	2.89	2.37

(b) Tie cable natural length

	Tie cable length
Upper limit (mm)	70.0
Optimum length (mm)	63.67

The objective function is the RMS error between the deformation shape and an ideal deformation shape, which is defined as follows:

$$v = u^2/16 \tag{6}$$

where u is the longitudinal coordinate and v is the bending deformation.

The rib is modeled by using 80 beam elements, such that the rib between each node in Fig. 2 is equally divided into 10 beam elements. The tie cable is modeled as a single cable element. The root of the rib is simply supported and the bottom end of the tie cable is fixed in the height direction but is free to move in the lateral direction. The hoop cable tension values are given as the equivalent nodal force, as listed in Table 1. The tie cable tension is given as a reaction force resulting from the rib deformation, where the Young's modulus of the rib and the cable stiffness are set to constants as 70 GPa and 2000 N, respectively.

In the optimization problem, the beam height is treated as a design variable, where the beam cross section is assumed to be a rectangular shape and the beam width is set to be constant at 5 mm. The design variables are allocated such that the beam elements between each node have the same beam height except for the two ends. Both ends allocate two variables such that the elements between the nodes are divided into two equal parts, and then each variable allocates each of the five elements on the left- and right-hand sides. Hence, the number of the beam height variables is 10. In addition, the natural length of the cable element is treated as a design variable. The length indirectly affects the rib deformation shape to change the cable tension that is represented as the reaction force. As a result, the total number of design variables is 11.

For numerical stability, the lower limits of the rib thicknesses are imposed as listed in Table 2(a). In addition, the upper limit of the tie cable natural length is given as listed in Table 2(b) to avoid slackening of the tie cable. It is confirmed that no limits are active under this optimization or the following multiobjective optimization problems.

Using the simple model, the RMS error minimization design is obtained as shown in Table 2. The obtained RMS error is 0.0288mmRMS, which satisfies the design requirement of 0.05mmRMS [2].

The structural model described herein is different from that in the original study [2]. In the original study, the tie cable was not modeled as the tie cable element. The cable tension was given as the nodal force at rib node 4 in the vertical direction

and the lateral direction was fixed at the rib tip. The optimization was performed to minimize RMS error, as well as to reduce the reaction force at the tip. It is difficult to use this model for evaluating the effect of variations of the cable tension on the rib deformation, which is why the current study updates the structural model to that shown in Fig. 2. The difference between the obtained results and the previous results [2] is very small. The RMS error was 0.037mmRMS and the difference of the rib thickness distribution was small. For the above reasons, this structural model is considered adequate for the current purpose.

3.1. Formulation of multiobjective optimization problem

The deformation RMS error minimization is not the only design requirement; the RMS error sensitivity is also required in order to solve the design problem. This study focuses on the RMS error sensitivity with respect to the cable tension force as the performance measure of the robustness. The rib shape is changed by the cable tension. The design is called robust when the sensitivity is small.

The robustness or adjustability are investigated by formulating the design problem as a multiobjective optimization problem. The objective functions are described as follows:

$$f_1 = \text{Deformation RMS error from the ideal deformation shape (mm)} \quad (7)$$

$$f_2 = \text{RMS error sensitivity with respect to tension of the tie cable at node 4 (mm/N)} \quad (8)$$

$$f_3 = \text{RMS error sensitivity with respect to tension of the outermost hoop cable at node 8 (mm/N)} \quad (9)$$

where sensitivity with respect to the cable tension is evaluated by the following forward difference [10] :

$$\frac{\partial \mathrm{RMS}(\boldsymbol{x}, \boldsymbol{z})}{\partial z_i} \approx \frac{\mathrm{RMS}(\boldsymbol{x}, \boldsymbol{z} + \Delta z_i) - \mathrm{RMS}(\boldsymbol{x}, \boldsymbol{z})}{\Delta z_i} \quad (10)$$

where $\boldsymbol{z}$ denotes the design parameters as the cable tension. minimization of f_2 or f_3 corresponds to the robust design.

3.2. Verification sequence

As described above, the design requirement for the RMS error corresponding to f_1 is set as less than 0.05mmRMS [2] . However, the reference values of the RMS error sensitivity have not been referred. Therefore, the design verification is performed in the following sequence to clarify the effect of variation of cable tension on the rib deformation.

Step 1 A single-objective optimization problem to minimize the deformation RMS error f_1 is obtained first. The optimum design listed in Table 3 is used as the reference design. Values of the objective functions on the reference design are listed in Table 2.

Step 2 Two-objective optimization problems consisting of f_1 and f_2 or f_1 and f_3 are performed. The aspiration levels are parametrically changed to obtain a highly diverse and uniformly distributed Pareto set. Then, it is evaluated in terms of how much the sensitivity is improved by sacrificing the RMS error within the allowable range.

Step 3 Finally, three-objective optimization problem considering all objective functions f_1, f_2, and f_3 is evaluated, where the aspiration levels are limited to only the range of interest from the previous step. Then, the effect of variations of cable tension on the rib deformation is discussed.

Table 3. Reference design as RMS error minimization design

Objective	f_1 (mmRMS)	f_2 (mm/N)	f_3 (mm/N)
Reference value	0.0288	66.0	27.8

Investigating only a limited number of three-objective optimum designs using properly determined aspiration levels is the major advantages of STOM for design verification. It is also effective to save the computational cost.

4. Design Verification

The respective initial Pareto solutions obtained from the two objective function problems of this example are shown in Figs. 5 and 6, where the two objectives are to minimize f_1 and f_2 and f_1 and f_3, respectively. The lower rightmost Pareto solution in both Figs. 5 and 6 corresponds to the reference point as listed in Table 3. Both Pareto curves show the trade-off relationship between f_1 and f_2 and f_1 and f_3. That is, the RMS error increases as the RMS error sensitivity decreases. Within the allowable range of an RMS error lower than 0.05mmRMS, f_2 and f_3 decrease by as much as approximately 20 mm/N and 3 mm/N, respectively.

These Pareto points are obtained by parametrically changing the aspiration levels, where the f_1–f_2 and the f_1–f_3 problems use eight and six aspiration levels, respectively, as shown in Figs. 5 and 6, respectively. These points are initially selected from the reference points; later, the aspiration level can set as close to the Pareto point as desired. The dotted line in Fig. 6 indicates the connecting line from the ideal point to the aspiration level, showing that the found Pareto solution lies on the line. This corresponds to the characteristics of the STOM shown in Fig. 4.

Then, the three-objective design problem to minimize f_1, f_2, and f_3 is solved by setting the aspiration levels, referring to the results of the two-objective problems above. The Pareto solutions plot in f_2–f_3 space is shown in Fig. 7. The values correspond to the RMS error, f_1. The upper rightmost point of 0.029mmRMS corresponds to the reference design listed in Ta-

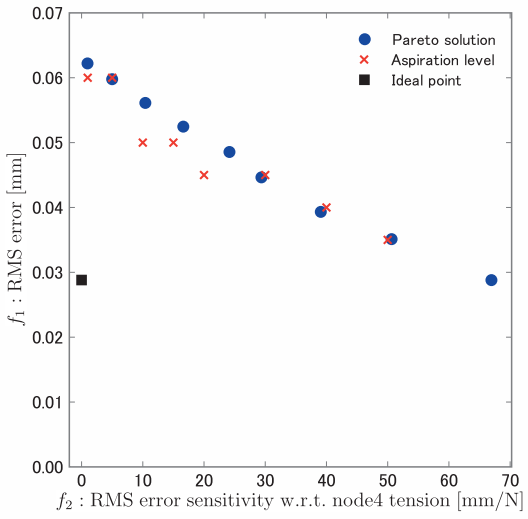

Fig. 5. Pareto set distribution in f_2–f_1 space for the two-objective function problem

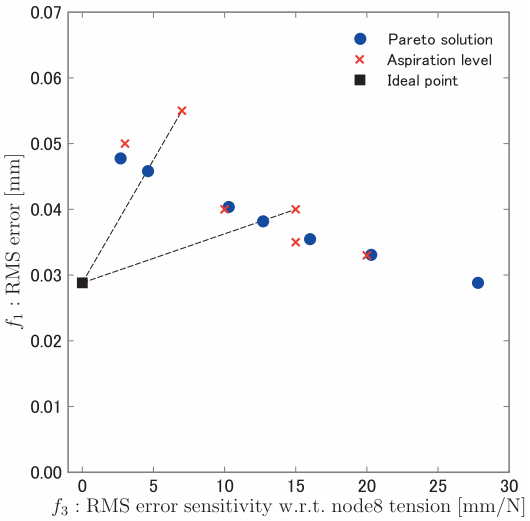

Fig. 6. Pareto set distribution in f_3–f_1 space for the two objective function problem

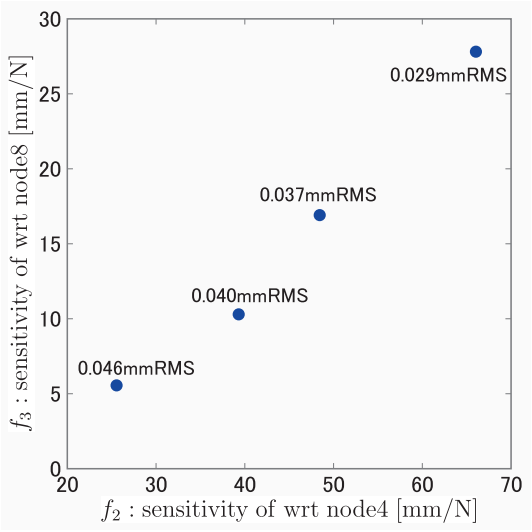

Fig. 7. Pareto solution for the three-objective optimization problem

ble 2. The Pareto solution distribution in Fig. 7 shows that f_2 and f_3 have a strong correlation and the possibility of improvement of f_2 and f_3 by sacrificing the RMS error f_1 within the allowable range.

From this result, it is useful to obtain robust designs that minimize both RMS error sensitivity terms with respect to the tie cable and the outermost hoop cables.

To investigate the relationship between the RMS error sensitivity and the nodal deformation by the variation of cable tension, each nodal displacement sensitivity with respect to the outermost hoop cable or tie cable tensions are investigated in Fig. 8 and Fig. 9. In Fig. 8, the sensitivity is small in the vicinity of tie cable and ends of the root. It is because the root of the rib is simply supported and vicinity of node4 is affected by the reaction force of the tie cable. In contrast, the sensitivity is high in the outermost hoop cable, because node8 is free end. On the other hand, Fig. 9 shows the nodal displacement sensitivity with respect to tie cable. The sensitivity increases monotonically.

Both Fig. 8 and Fig. 9 shows the each nodal displacement

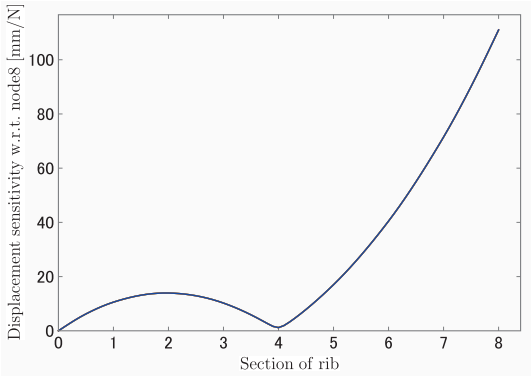

Fig. 8. Nodal displacement sensitivity with respect to the outermost hoop cable tensions

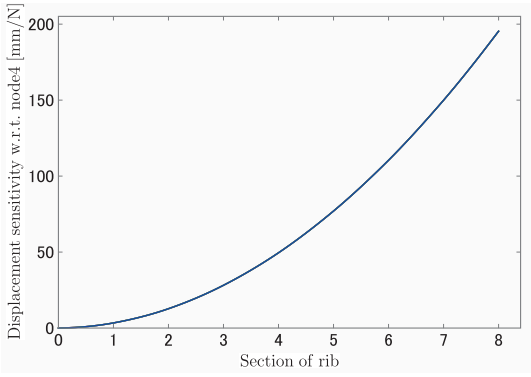

Fig. 9. Nodal displacement sensitivity with respect to tie cable tension

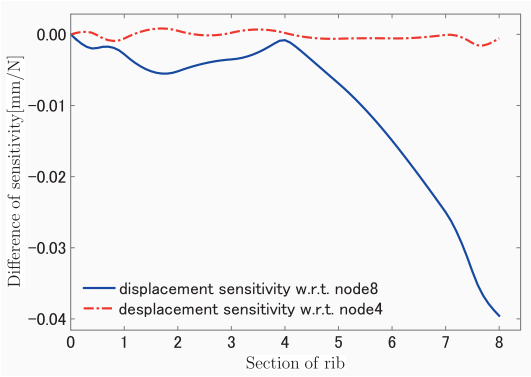

Fig. 10. Difference of nodal displacement sensitivity between the reference design and the lowermost point

sensitivity for all four Pareto solutions. However, there is little difference between the obtained Pareto solutions, so the difference cannot be seen in both figures.

To investigate the differences of each nodal displacement sensitivity, the difference between reference design point and the lowermost point of 0.046mmRMS are shown investigated. The difference between the sensitivity of the reference design point and that of the the lowermost point of 0.046mmRMS in shown in Fig. 10 . Fig. 10 shows the difference of both displacement sensitivity with respect to tie cable and outermost hoop cables. The sensitivity for the point of 0.046mmRMS is smaller than reference design point, This result confirms to achieve robustness to variation of the tie cable and the outermost hoop cable tensions.

5. Conclusion

This study verifies the structural design considering uncertainties of a space reflector structure consisting of radial ribs and hoop cables by using the multiobjective optimization method. Deformation RMS error with respect to the accuracy of rib deformation and RMS sensitivities with respect to cable tension are selected as objective functions to investigate the trade-off between the deformation accuracy and variations of the cable tension. As multiobjective optimization, STOM is applied as numerically efficient method.

In this study, a three-step approach is adopted. First, single-objective optimization is performed to minimize the RMS error; the obtained optimum design is regarded as the reference value. Then, two sets of two-objective optimization, one including the RMS error and the other including the sensitivity, are performed to investigate the Pareto set distributions as the robust optimum solutions. Finally, the Pareto solutions of a three-objective optimization problem are obtained to investigate the trade-off relationship between the robust design candidates. In addition, variations of nodal displacement sensitivity are investigated to confirms the archived robustness of the robust designs.

Acknowledgment

This study is partially supported by JSPS KAKENHI 26249131.

References

1) Higuchi, K., Kishimoto, N., Meguro, A., Tanaka, H., Yoshihara, M. and Iikura, S.: Structure of high precision large deployable reflector for space VLBI (very long baseline interferometry), Proceedings of 50th AIAA/ASME/ASCE/AHS/ASC Structures, Structural Dynamics, and Materials Conference, AIAA-2009-2609 (2009), pp. 1-9.
2) Tanaka, H, Akita, T., Kogiso, N., Ishimura, K., Sakamoto, H., Ogi, Y., and Miyazaki, Y.: A design method for a space antenna structure consisting of radial ribs and hoop cables, Proceedings of 24th JSME Computational Mechanics Conference CMD2011, No. 2326 (2011), pp. 687-688. (in Japanese)
3) Miyazaki, Y., and Tanaka, H.: Elastica solution for simplified model for a space antenna structure consisting of radial ribs and hoop cables, Proceedings of 24th JSME Computational Mechanics Conference CMD2011, No. 2327 (2011), pp. 689-690. (in Japanese)
4) Nakayama, H., and Sawaragi, Y.: Satisficing trade-off method for multiobjective programming, Lecture Notes in Economics and Mathematical Systems, Vol. 229 (1984), pp. 113-122, doi:10.1007/978-3-662-00184-4_13
5) Nakayama, H., Kaneshige, K., Takemoto, S., and Watada, Y.: An application of a multi-objective programming technique to construction accuracy control of cable-stayed bridges, European Journal of Operational Research, Vol. 87, No. 3 (1995), pp. 731-738, doi:10.1016/0377-2217(95)00241-3
6) Okamoto, T., Hanaoka, Y., Aiyoshi, E., and Kobayashi, Y.: A buffer material optimal design in the radioactive wastes geological disposal using the satisficing trade-off method and the self-organizing map, Electrical Engineering in Japan, Vol. 187, No. 2 (2014), pp. 17-32, DOI: 10.1002/eej.22634
7) Toyoda, M. and Kogiso, N.: Robust multiobjective optimization method using satisficing trade-off method, Journal of Mechanical Science and Technology, (accepted for publication).
8) Kogiso, N, Kodama, R. and Toyoda, M.: Reliability-based multiobjective optimization using the satisficing trade-off method, Journals of the Japan Society of Mechanical Engineers, Vol. 1, No. 6 (2014), p. DSM0063, doi: 10.1299/mej.2014dsm0063
9) Nakayama, H.: Trade-off analysis using parametric optimization techniques, European Journal of Operational Research, Vol. 60, No. 1 (1992), pp. 87-98, doi:10.1016/0377-2217(92)90336-8
10) Kogiso, N., Tanaka, H, Akita, T., Ishimura, K., Sakamoto, H., Ogi, Y., Miyazaki, Y., and Iwasa, T.: Comparison of computation accuracy in FEM analysis for a space antenna structural design, Proceedings of 24th JSME Computational Mechanics Conference CMD2011, No. 2328 (2011), pp. 691-693. (in Japanese)
11) Ang, A. H.-S. and Tang, W. H.: Probabilistic concepts in engineering design, basic principles, (1975), Wiley.
12) Beyer, H. and Sendhoff, B.: Robust optimization – a comprehensive survey, Computer Methods in Applied Mechanics and Engineering, Vol. 196, No. 33-34 (2007), pp. 3190-3218, doi:10.1016/j.cma.2007.03.003
13) Jeong, M. J., Dennis, B. H., and Yoshimura, S.: Multidimensional clustering interpretation and its application to optimization of coolant passages of a turbine blade, Journal of Mechanical Design, Vol. 127, No. 2, (2005), pp. 215-221, doi:10.1115/1.1830047
14) Kohira, T., and Amano, K.: Knowledge discovery for car-body weight reduction with multidisciplinary design optimization and trade off analysis, IEEJ transactions on Electronics, Information and Systems, Vol. 134, No. 9 (2014), pp. 1348-1354, (in Japanese) doi:10.1541/ieejeiss.134.1348
15) Mittinen, K. M.: Nonlinear multiobjective optimization, (2004), Kluwer Academic Publishers.
16) Obayashi, S., and Sasaki, D.: Visualization and data mining of Pareto solutions using self-organizing map, Lecture Notes in Computer Science, Vol. 2632 (2003), pp. 796-809, doi:10.1007/3-540-36970-8_56
17) Oyama, A. Nonomura, T and Fujii, K.: Data mining of Pareto-optimal transonic airfoil shapes using proper orthogonal decomposition, Journal of Aircraft, Vol. 47, No. 5 (2010), pp. 1756-1762, doi:10.2514/1.C000264
18) Park, G., Lee, T., Lee, K., and Hwang, K.: Robust design: an overview, AIAA Journal, Vol. 44, No. 1 (2006), pp. 181-191, doi:10.2514/1.13639